basis for the data determined in Fig. 2 may be found in the included Appendix. Fig. 2 is a useful tool in selecting values for G_F and G_B. The x axis of the graph of Fig. 2 represents unsaturated forward Raman gain. The left y-scale of the graph of Fig. 2 represents input power per channel to fiber 115. The right y-scale of Fig. 2 reports the corresponding four-wave mixing-induced cross talk at the end of the whole link of 25 spans assuming that G_B provides the remainder of the 15 dB that G_F does not provide. To get this crosstalk, individual contributions from each span are added.

a1

Please replace the paragraph beginning on page 11, line 23, with the following:

Fig. 4 shows the Rayleigh backscattering product caused by either the co-propagating pump or counter-propagating pump. This product is computed using the techniques disclosed in P.Hansen et al., *IEEE Photon. Tech. Lett.*, Vol.10, No1 (1998), p. 159, the contents of which are herein incorporated by reference. To evaluate the backscattering product suppression for a given configuration of Raman amplifier 113, one separately determines the suppression levels for the forward and backward gains using the values given by Fig. 4 for the number of spans in the link. Then, the double Rayleigh back scattering noise levels contributed by the forward and backward gain are computed given the suppression levels and the signal level at the output level of Raman amplifier 113. These noise levels are added and compared to the signal level to obtain the double Rayleigh backscattering suppression level. In general, double Rayleigh backscattering suppression of greater than 30 dB is typically required. For our previous example system where G_F= 5.5 dB and G_B= 9.5 dB, the double Rayleigh backsckattering suppression is approximately 37.5 dB.

a2

Please add the following appendix after the claims:

APPENDIX

Interaction of Four-Wave Mixing and Distributed Raman Amplification

An analysis of four-wave mixing build up in presence of distributed Raman amplification is presented here. Co- and counter-propagating pumping schemes have been considered. Under proper conditions, the induced cross talk is demonstrated to be dependent only on total Raman gain, no matter which the balance between co- and counter-propagating pumps is. Taking into account the different noise properties of the two pumping schemes, the co-propagating one is established to be more effective in reducing four-wave mixing impairments in a WDM system.

a3

Introduction

Though the light amplification by means of the Raman effect in optical fibers is known [1][2], only recently distributed Raman amplification has been considered in commercial systems. The reason of this revival lies both in the present availability of laser sources powerful enough to obtain an acceptable gain with practical pump modules and in the need of far increasing capacity of optical system. In the recent years hybrid systems with distributed Raman amplification (i.e. in transmission fiber) and erbium doped fiber amplifiers (EDFA) appeared [3][4]. This combination is employed to reduce the non-linear impairments in WDM systems. The EDFAs are used to control the signal power input to the fibers, while the noise properties of the Raman amplification make possible to keep it low, so that the non linear impairments lessen. The majority of these systems employ only counter propagating pump schemes, despite the worst noise performance [1][2], because common sense considerations suggest the co-propagating scheme may be detrimental for nonlinear propagation impairments. However, no detailed analysis of the interaction of Raman amplification and non linear propagation WDM effect has been provided. The aim of this appendix is to fill this gap for what concerns four-wave mixing (FWM).

a3

1. System Modeling.

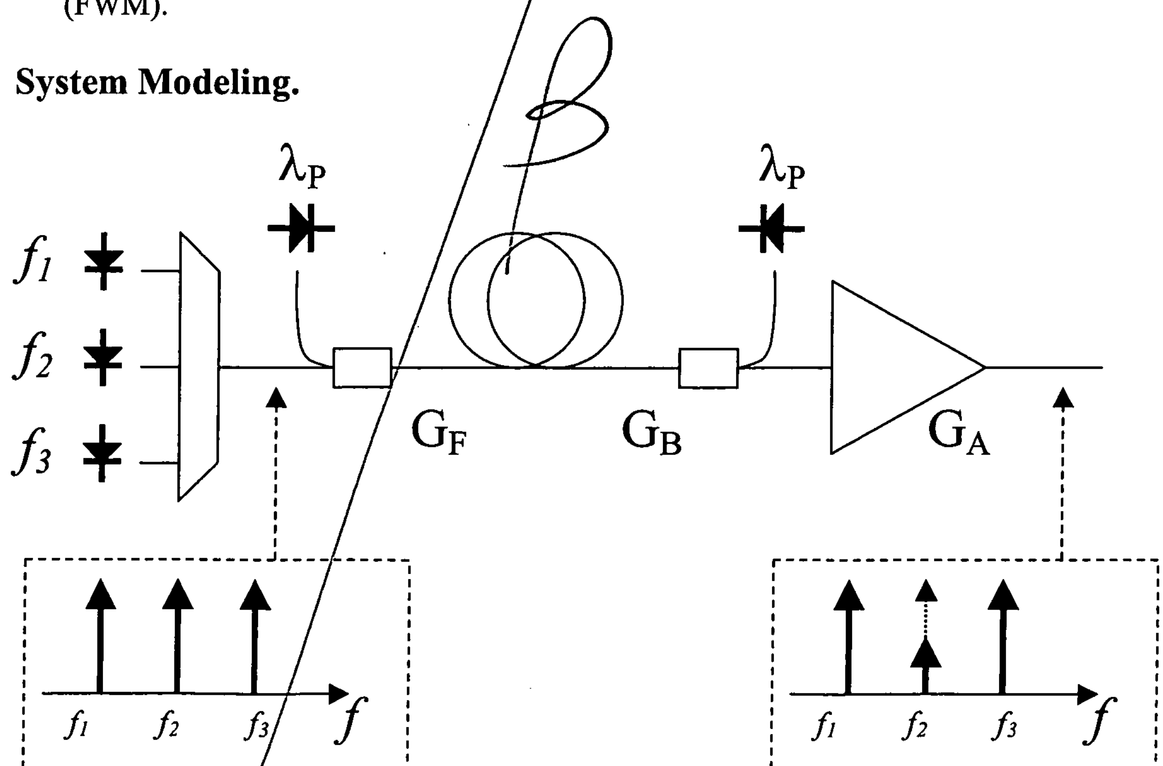

Figure 1. Layout of the system under study.

In order to evaluate how distributed Raman amplification affects FWM, the system sketched in Figure 1 has been considered. It consists in a single fiber span with loss α and length L, followed by an EDFA. Two lasers at the proper wavelength (100 nm apart from the signals) are injected at the two ends of the fiber, generating Raman amplification. The input signals are subjected to a forward and a backward gain (G_f and G_b) defined as the Raman gain experienced switching on and off the corresponding laser pumps [1]. The EDFA's gain G_A ensures the "transparency condition"

$$G_A \cdot G_B \cdot G_F \cdot \exp(\alpha_s L) = 1 \tag{1}$$

The power evolution of the channels in presence of both forward and backward Raman pumping, under the assumption that pump depletion is negligible, is described by the formula [1]:

$$\frac{dP_{ch}(z)}{dz} = -\alpha_S P_{ch}(z) + \frac{1}{L_{eff,p}}\left(\ln(G_F)e^{-\alpha_p \xi} + \ln(G_B)e^{-\alpha_p(L-\xi)}\right)P_{ch}(z) \tag{2}$$

where α_P and α_S are the fiber loss at pump and at signal wavelength respectively, $L_{eff,P} = (1-\exp(-\alpha_P L))/\alpha_P$ is the effective length of the pump, G_F and G_B are the forward and the backward Raman gains, respectively. It is worth noting that this formulation depends only on the gains regardless of fiber-characteristic parameters as the effective area or the pump power.

Together with amplification, Raman ASE is generated within the fiber. According to Aoki [1], the Raman ASE can be effectively described via integration of the formula:

$$P_{ASE,R} = 2h\upsilon\Delta\upsilon \int_0^L r_0 N_p(\xi)\exp\left(-\alpha_s(L-\xi) + \int_\xi^L r_0 N_p(\eta)d\eta\right)d\xi \tag{3}$$

where $h\nu$ is the photon energy, $\Delta\nu$ is the appropriate bandwidth over which the noise power is measured, r_0 is the Raman gain coefficient. The pump photon number $N_p(z)$ is proportional to the pump power and, in the unsaturated gain approximation, is described by the formula:

$$N_P(z) = \frac{1}{r_0}\frac{1}{L_{eff,P}}\left(\ln(G_F)e^{-\alpha_p z} + \ln(G_B)e^{-\alpha_p(L-z)}\right) \tag{4}$$

The ASE generated within the EDFA can be evaluated by the well-known formula:

$$P_{ASE,EDFA} = 2h\upsilon\Delta\upsilon(G_A - 1)n_{sp} \tag{5}$$

where n_{sp} is the population-inversion factor [10].

Three CW co-polarized and equally spaced channels propagates through the fiber. Interacting via the fiber non-linearity, they generate 9 FWM products, but only the product lying under the central channel will be considered in the following.
To analyze FWM generation, a common procedure can be followed, taking into account only CW signals, so that the group velocity dispersion (GVD) and the cross-phase modulation (XPM) can be considered as secondary effects and then ignored. This greatly simplifies the formalism, and the evolution of the three interacting channels and of the generated FWM product along the amplified fiber can be written in the form

$$\begin{aligned} \frac{dA_F(z)}{dz} &= \frac{1}{2} g(z) A_F(z) + i\gamma A_p(z) A_q(z) A_r^*(z) \exp(i\Delta\beta z) \\ \frac{dA_p(z)}{dz} &= \frac{1}{2} g(z) A_p(z) \\ \frac{dA_q(z)}{dz} &= \frac{1}{2} g(z) A_q(z) \\ \frac{dA_r(z)}{dz} &= \frac{1}{2} g(z) A_r(z) \end{aligned} \tag{6}$$

where A_F, A_p, A_q, A_r are the complex envelopes of the electrical field at frequencies f_F, f_p, f_q, f_r respectively ($f_F=f_p+f_q-f_r$),

$$g(z) = -\alpha_S + \frac{1}{L_{eff,p}}\left(\ln(G_F)e^{-\alpha_p\xi} + \ln(G_B)e^{-\alpha_p(L-\xi)}\right) \tag{7}$$

is the gain experienced by the considered channels, and $\Delta\beta$ is the well-known phase-mismatch parameter [11]:

$$\begin{aligned} \Delta\beta &= \beta_p + \beta_q - \beta_r - \beta_F \\ &= \frac{2\pi\lambda^2}{c}(f_p - f_r)(f_q - f_r)\left[D(\lambda) - \frac{\lambda^2}{c}\left(\frac{f_p + f_q}{2} - f\right)\frac{dD}{d\lambda}\right] \end{aligned} \tag{8}$$

Following Aoki [1], the Raman gain can be supposed constant over a wavelength range wide enough to contain all channels. Introducing the integrated gain:

$$G_\xi(z) = \exp\left(\int_0^\xi g(z')dz'\right) \tag{9}$$

the solution of equation (6) is [5]:

$$A_F(z) = i\gamma \frac{D_{pqr}}{3} A_p(0) A_q(0) A_r^*(0) \sqrt{G(z)} \int_0^z G(\zeta) e^{i\Delta\beta\zeta} d\zeta \tag{10}$$

Equation (10) evaluated at L (fiber length) gives the electrical field of the FWM product at the end of the fiber. Supposing that the channels have the same power P_{ch} at the fiber input, the FWM induced cross talk can be written as:

$$X_F(L) = \frac{P_F}{P_{ch}} = \left(\gamma \frac{D_{pqr}}{3}\right)^2 P_{ch}^2 \left| \int_0^L G(\zeta) e^{i\Delta\beta\zeta} d\zeta \right|^2 \tag{11}$$

To keep discussion simple, some assumptions have been made. First, there is no pump depletion that may invalidate equations (2) and (4) and cause cross talk between WDM channels [5] through the co-propagating pump. This states a limit in the allowable forward gain, but this limit depends also on channel and pump power. To avoid considering this dependence, the effect is neglected. The other effect neglected in this report is the interference caused by Rayleigh scattering [8] setting too an upper limit in allowable gain. Discussion on these topics is beyond the scope of this report.

2. ASE Noise in Hybrid Systems

Figure 2 reports the total noise power over a 0.5 nm bandwidth at the EDFA's output, calculated according to the formula

$$P_{ASE} = G_A P_{ASE,R} + P_{ASE,EDFA} \tag{12}$$

and considering a 6 dB noise figure for the EDFA. The contour plot clearly shows the improvement in noise performances due to the Raman amplification, as the noise power decreases for higher Raman gain. It is also worth noting that the main contribution to the noise, for the same total Raman amplification ($G_F G_B$), is due to the backward pump. As a matter of fact, a 1 dB increase in G_F induces a 1 dB reduction in the total ASE power. It follows that forward pumping allows obtaining a higher signal-to-noise ratio.

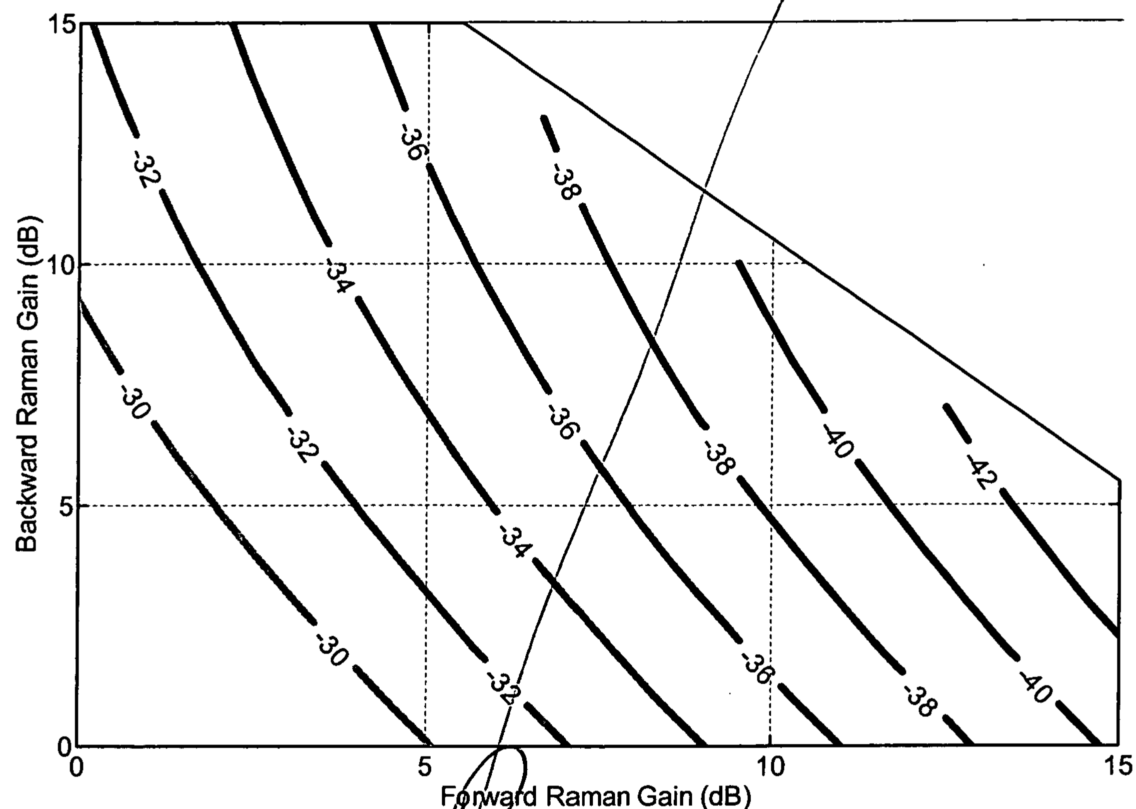

Figure 2. Total noise power (dBm) over 0.5 nm bandwidth (Δv) generated by a Raman amplified span followed by an EDFA with a 6 dB noise figure. Fiber attenuation is α_P=0.3 dB/km, and α_S=0.2 dB/km at the pump and signal wavelengths, respectively. Fiber length is L=100 km.

3. FWM Dependence on Pumping Scheme in Raman Distributed Amplifiers.

When dealing with non-linear propagation effects (as FWM), it is customary to define an "effective length" $L_{eff} = \int_0^L G(z)dz$ that enables an approximated evaluation of the intensity of the non-linear effects [11]. The dependence of the effective length (in the unsaturated gain approximation) from both the forward and the backward Raman gains is reported as a contour plot in Figure 3. As expected, the effective length mainly depends on the forward gain, while the backward gain contributes only negligibly. It is worth noting that, contrary to the case of a span without Raman amplification, $L_{eff} > L$ for large gain. This happens because G(0)=1, i.e. the effective length is referred to the input power.

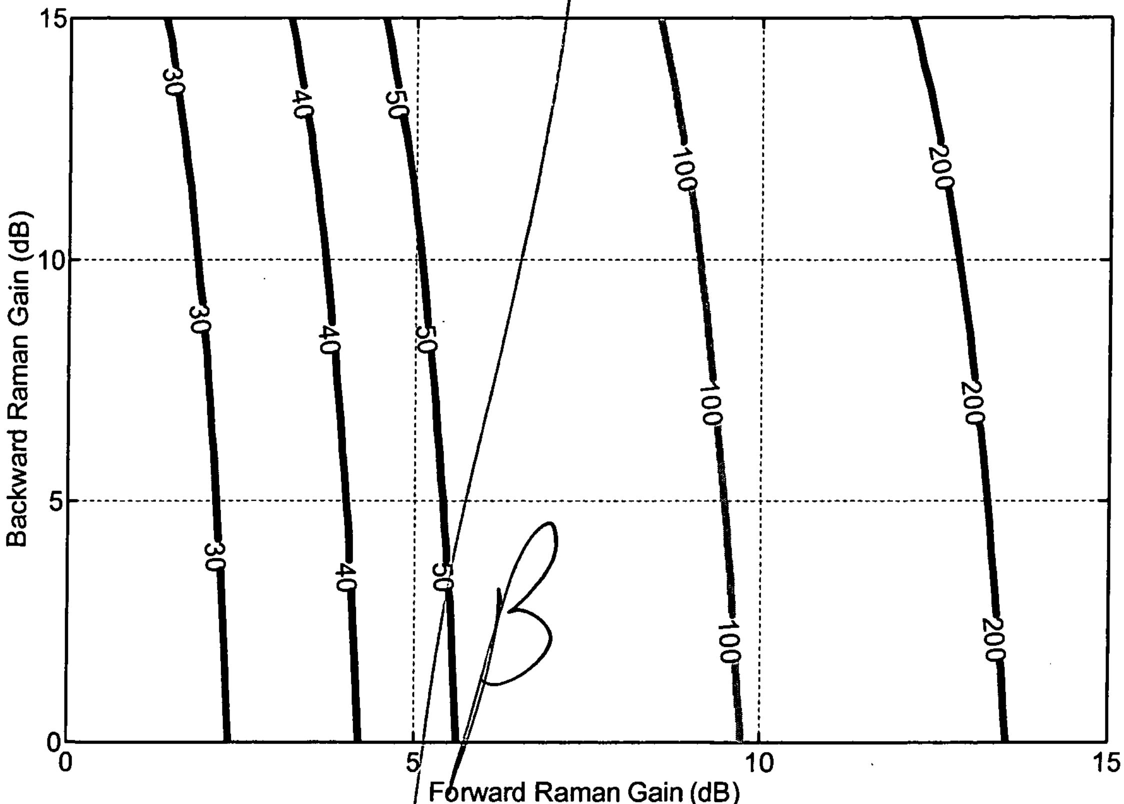

Figure 3. Effective length in a 100-km-long fiber span with forward and backward Raman amplification. Fiber attenuation is α_P=0.3 dB/km, and α_S=0.2 dB/km at the pump and signal wavelengths, respectively.

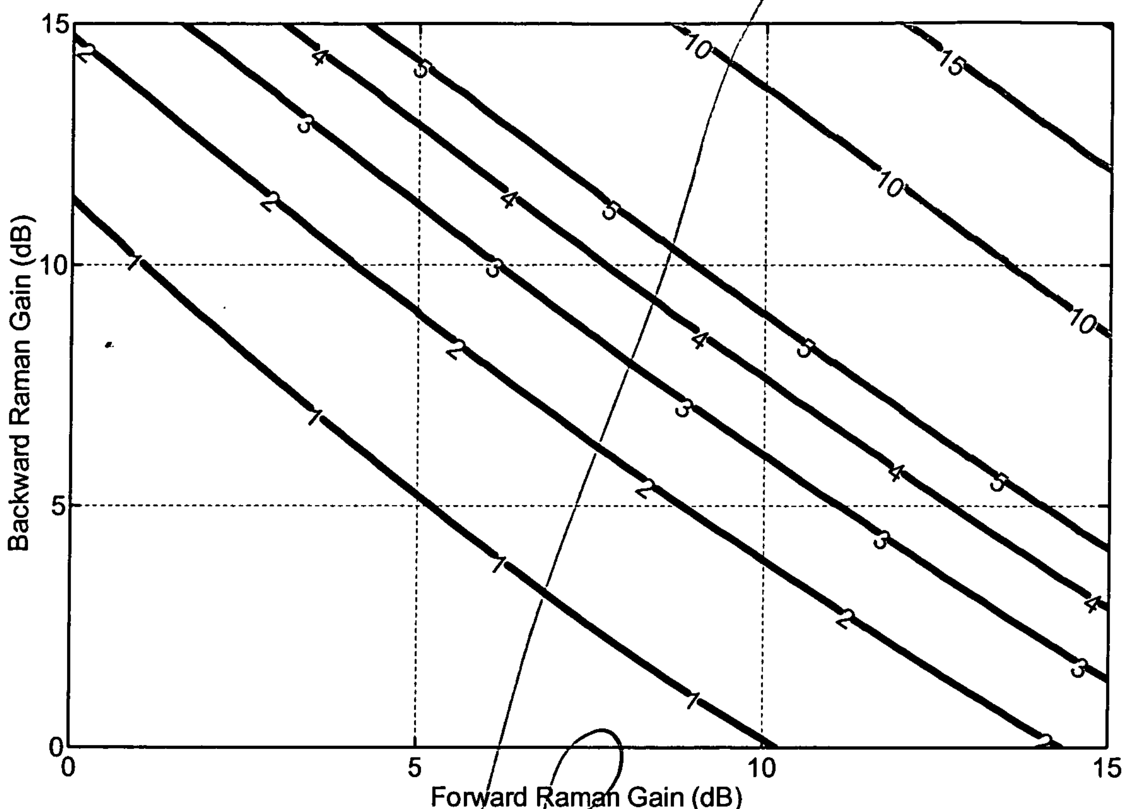

Figure 4. FWM cross talk dependence on forward and backward Raman gains for the central one of 3 CW channels 50 GHz spaced. A TW-RS fiber is considered with a dispersion of 4.5 ps/nm, α_P=0.3 dB/km, α_S=0.2 dB/km and a length of environ 100 km. The FWM cross talk is reported in dB relatively to the case of no Raman amplification (the origin in the plot).

However, surprising results can be achieved when the FWM equation (11) is numerically integrated. Figure 4 reports as a contour plot the FWM cross talk for various choices of forward and backward Raman gains. The cross talk is reported in dB relatively to the case of no Raman amplification (the origin in the plot). This way the plot is independent from the effective area of the fiber. Being the result strongly dependent on the product $\Delta\beta \cdot L$, the length L has been chosen in order to have

$$\Delta\beta \cdot L = (2n+1)\pi \tag{13}$$

This is a worst case, because the FWM field has the maximum amplitude, as will be shown in the following. Figure 4 clearly shows that the FWM depends only from the total Raman gain ($G_F G_B$) no matter what the balance between forward and backward pumping is. This is totally different from what could be expected from "effective length" consideration, as appears evidently comparing Figure 4 with Figure 3.

These results can be explained observing that the FWM power is proportional to the square modulus of the Fourier integral of the gain evolution along the fiber. In formulas:

$$P_{FWM} \propto \left| \int_0^L G(z)\exp(i\,\Delta\beta\, z)\,dz \right|^2 \tag{14}$$

Repeatedly integrating by parts a series can be obtained, which converges under proper conditions:

$$\int_0^L G(z)\exp(i\,\Delta\beta\, z)\,dz = \sum_{n=1}^{\infty} \frac{G^{(n)}(0) - e^{i\Delta\beta L} G^{(n)}(L)}{(i\,\Delta\beta)^{(n+1)}} \tag{15}$$

For a mismatch $\Delta\beta$ large enough only the first term can be retained leading to the following approximation

$$\int_0^L G(z)\exp(i\,\Delta\beta\, z)\,dz \approx \frac{G(0) - e^{i\Delta\beta L} G(L)}{i\,\Delta\beta} = \frac{1 - e^{i\Delta\beta L} G_F\, G_B \exp(-\alpha_s L)}{i\,\Delta\beta} \tag{16}$$

Considering the worst case $\Delta\beta\, L = (2n+1)\pi$ the integral can be once more approximated as follows:

$$\int_0^L G(z)\exp(i\,\Delta\beta\, z)\,dz \approx \frac{1 + G_F\, G_B \exp(-\alpha_s L)}{i\,\Delta\beta} \tag{17}$$

demonstrating that, for a mismatch large enough, the FWM power depends only on the total Raman gain no matter how it is distributed between forward and backward pumping. To gain more physical insight, the expression for the FWM field evolution

$$A_F(z) = i\gamma \frac{D_{pqr}}{3} A_{p0} A_{q0} A^{*}_{r0} \sqrt{G(z)} \int_0^z G(\zeta) e^{i\Delta\beta\zeta}\, d\zeta \tag{18}$$

must be considered. This expression describes a curve in the complex plane, which is reported in Figure 5 and Figure 6. Raman forward and backward gains are chosen in order to obtain a plot suitable for exemplification. The distance from the origin of the last point of the curve is the square root of the FWM power. It is worth noting that the FWM power initially increases because the channel power raises rapidly, reaching very high values. When the channel power begins to fall, the curve in the complex plane begins to turn toward the origin, and the FWM power decreases. This means that the decrease of the channel power somehow cancels out the FWM build up in the first kilometers of fiber. This is true if the phase variation $\Delta\beta\, dz$ is large with respect to the local power variation (i.e. the local gain).

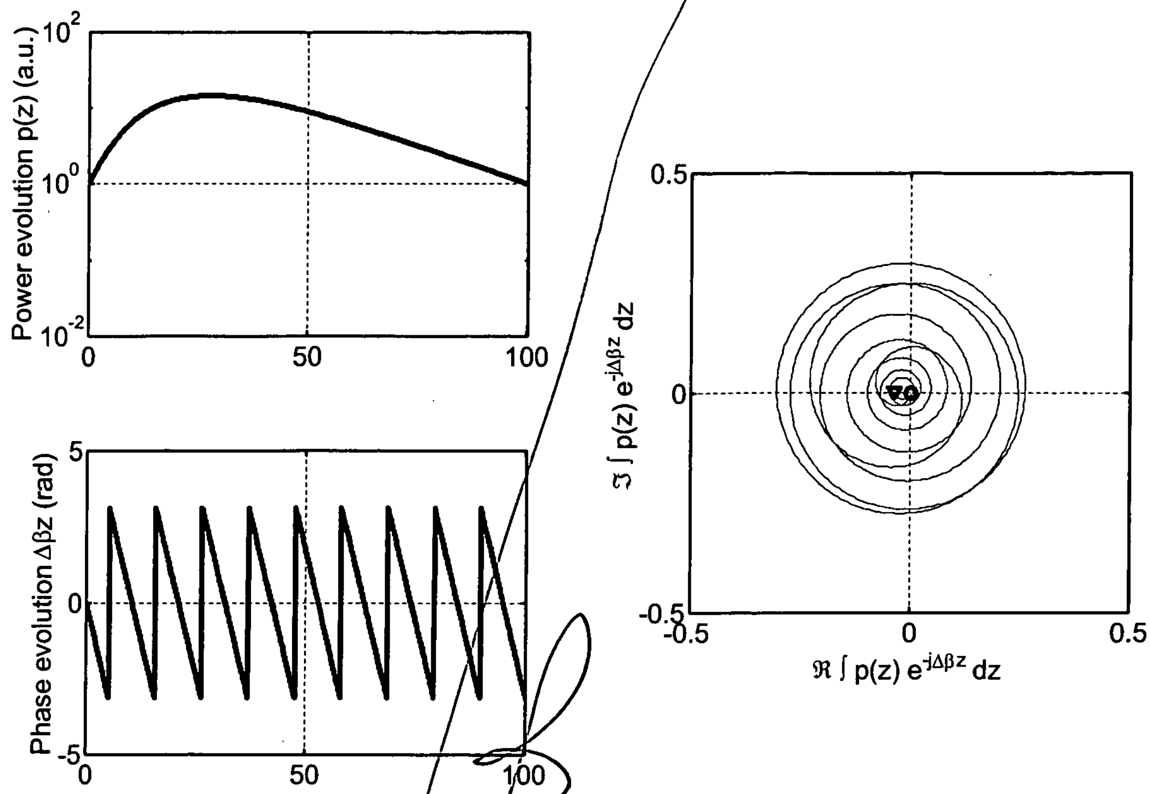

Figure 5. FWM field evolution along a Raman amplified fiber. Upper left graph reports the power evolution of the gain G(z) along the fiber, the lower left graph shows the phase evolution $\Delta\beta\, z$ (rad). The right hand graph represents the FWM field evolution in the complex plane. The circle corresponds to the start of the curve (z=0) while the triangle stands for the end of the curve (z=L). G_F=20 dB, G_B=0 dB, D=4.5 ps/nm, $\sqrt{(f_p - f_r)(f_q - f_r)} = 50$ GHz and L=100 km.

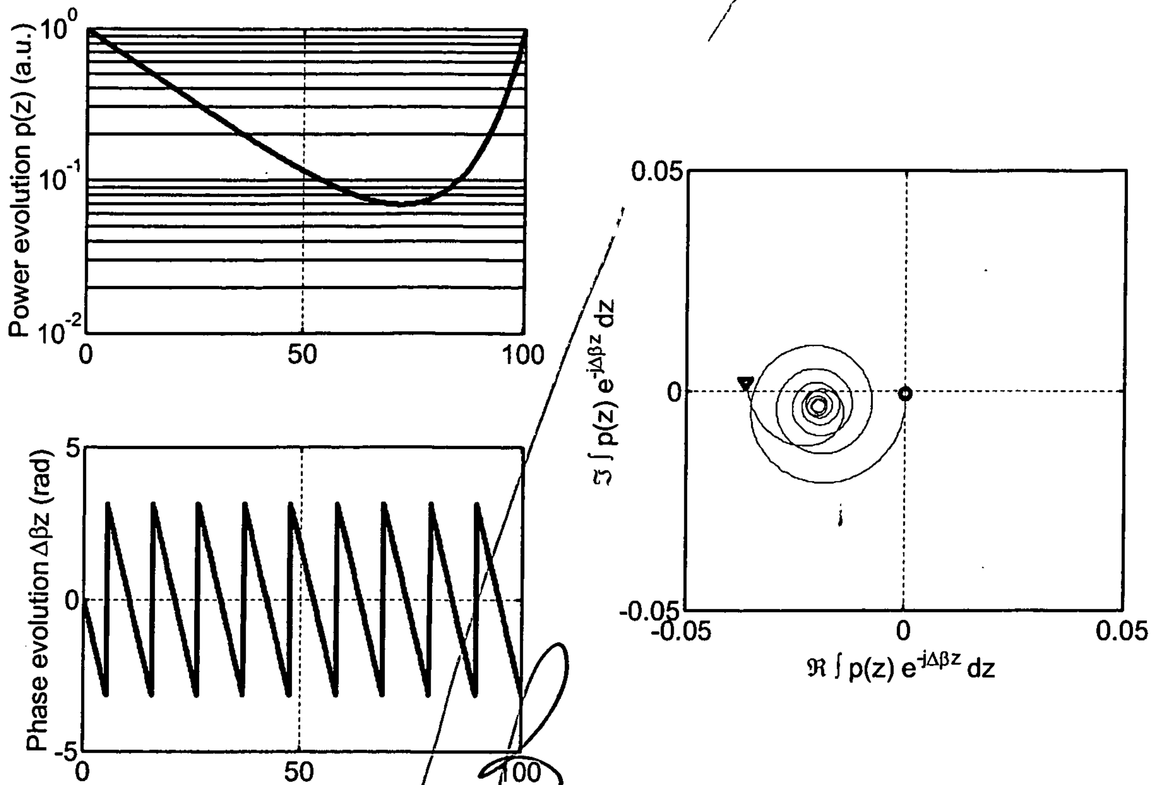

Figure 6. FWM field evolution along a Raman amplified fiber. Upper left graph reports the power evolution of the gain G(z) along the fiber, the lower left graph shows the phase evolution $\Delta\beta\, z$ (rad). The right hand graph represents the FWM field evolution in the complex plane. The circle corresponds to the start of the curve (z=0) while the triangle stands for the end of the curve (z=L). G_F=0 dB, G_B=20 dB, D=4.5 ps/nm, $\sqrt{(f_p - f_r)(f_q - f_r)} = 50$ GHz and L=100 km.

The complementary behavior is shown in Figure 6, where a backward gain equal to the span loss is used. In this case, the representative curve on the complex plane initially wraps up as a spiral, when channel power decreases. The following power rise induces the enlargement of the curve and therefore the increase of the FWM power.

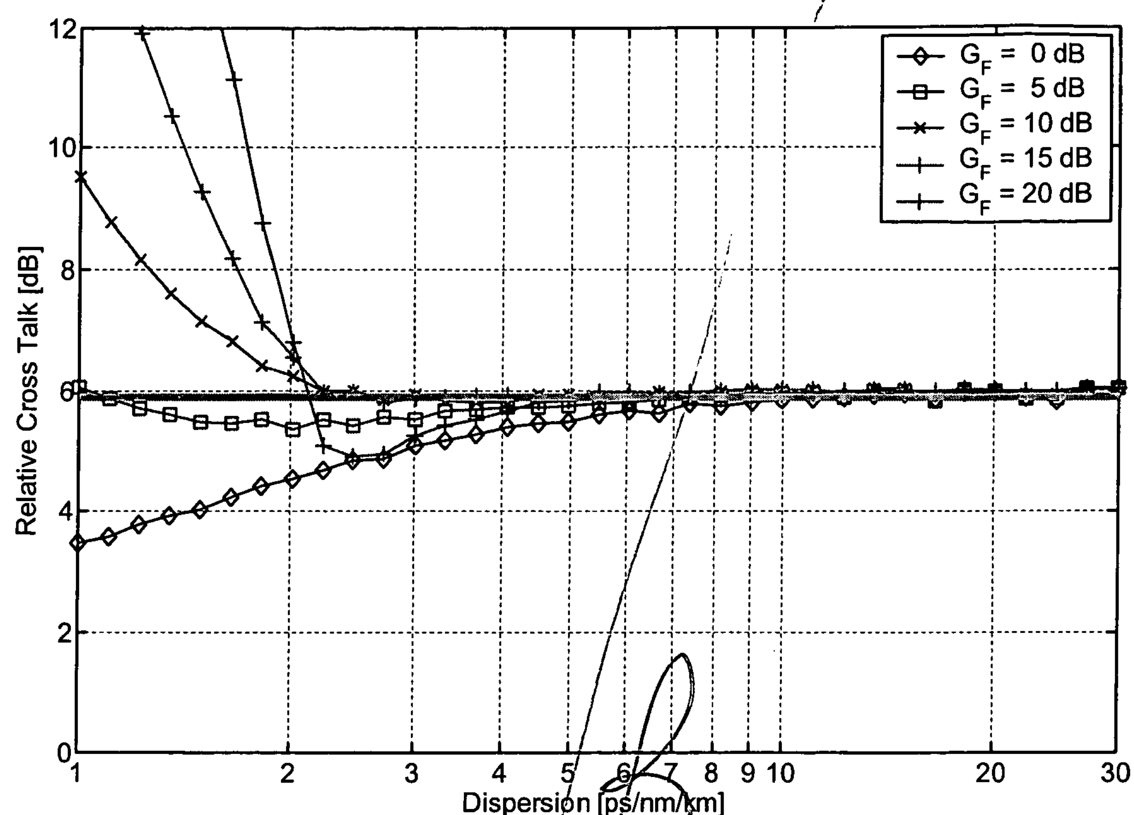

Figure 7 FWM cross talk for different dispersion values in a 100 km long fiber span with α_S=0.2 dB/km, α_P=0.3 dB/km and a total (i.e. $G_F G_B$) Raman gain of 20 dB. The cross talk is reported relatively to the case without Raman distributed amplification. Thin solid lines with symbols correspond to the exact solution for different balance between forward and backward gain. Thick dashed line corresponds to the approximation reported in the text. Channel spacing is 50 GHz.

With the aim to assess the validity range of the approximation shown in equation (17), the exact solution (equation (11)) has been solved for different values of chromatic dispersion and gain balance and compared with the approximate one. The fiber span is 100 km long with α_S=0.2 dB/km, and α_P=0.3 dB/km. The total distributed Raman gain has been chosen equal to 20 dB which is quite high and causes a noticeable cross talk increase. Solid lines with symbols correspond to the exact solution evaluated for different values of forward gain, provided the total Raman gain is kept fixed (i.e. $G_F G_B$= 20 dB). Being the cross talk strongly dependent on the product $\Delta\beta \cdot L$, for each dispersion value the fiber length has been varied over the range $[L-\pi/\Delta\beta\ ,\ L+\pi/\Delta\beta\ ]$, the equation (11) has been evaluated and the maximum value retained and reported in Figure 7. For the values of concern, the length variation is limited within 15 km. This procedure is mandatory because condition

(13) does not guarantee the worst case for D<4 ps/nm/km. Together with the length, α_S has also been varied in order to keep the span loss constant (varying G_B and G_F instead leads to results which slightly differ only for D<2 ps/nm/km). For small dispersion values, the gain balance has a noticeable effect, while increasing the dispersion value, all the lines tends towards the thick dashed one that represents the approximation (17). It is worth noting that for D>3 ps/nm/km the approximation error is less than 1 dB, and for D>2 ps/nm/km equation (17) provides an upper bound to cross talk increase. As expected, a higher forward gain provides a higher cross talk when dispersion is low and the approximation does not hold. The most unbalanced schemes (i.e. G_F=0 dB and G_F=20 dB) converge more slowly to the approximation as the gain evolution has a not negligible effect in this case. This also explains the little undershoot around D=2.5 ps/nm/km of the line corresponding to G_F=20dB.

A lower total Raman gain produces a lower growth in FWM cross talk and extends the validity range of the approximation towards lower dispersion values. Finally, it must be noted that the FWM scales with $\Delta\beta^2 \propto \left(D(f_p - f_r)(f_q - f_r)\right)^2$, so a doubling in channel spacing corresponds to a fourfold increase in the dispersion value. It follows that, for channel spacing greater than 50 GHz, the approximation fits even better.

4. Multi-Span System Considerations.

Figure 4 has been obtained considering a fixed input channel power, independently from the Raman gain. Nevertheless, Raman distributed gain is generally employed to reduce the channels' input power with the aim to keep non-linear propagation impairments low in multi-span systems. The reduction is achievable because the Raman distributed amplification can increase the SNR, as shown Figure 2. Being the Raman cross talk dependent on the square of the input channel power (eq. (11)) a reduction in the input channel power induces a double (in dB) reduction of the FWM cross talk. A 25-span system has been considered with D=4.5 ps/nm and requiring 12 dB of signal to noise ratio at the output ove a 0.5 nm bandwidth. FWM products generated in different spans are supposed to add incoherently, as the noise does, so that 10 spans show a cross talk 10 dB higher than a single one.

Using the formulas above, the FWM cross talk under the central channel can be evaluated keeping the output SNR fixed, and accordingly varying the channels' input power with the values of GF and GB. This leads to the contour plot Figure 8, which shows that the use of forward pumping is far more effective than the use of backward pumping in order to reduce the FWM cross talk. Indeed, FWM cross talk can be decreased by environ 17

dB using 10 dB of forward gain, while the same amount of backward gain can lessen the cross talk by 9 dB only.

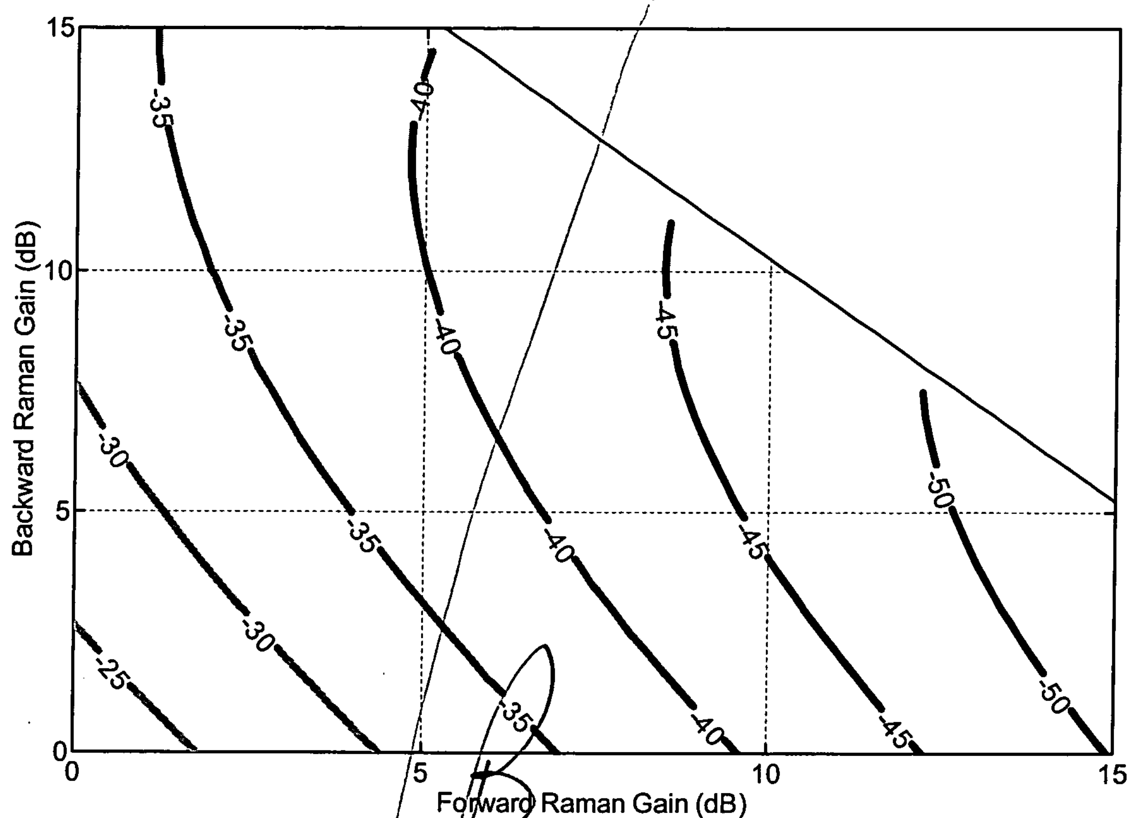

Figure 8. Four-wave-mixing cross-talk (dB) generated by 3 CW channels under the central one in a link of 25 Raman amplified spans of TWC fiber (D=4.5 ps/nm/km, A_{eff}=50 μm^2). Each fiber span is followed by a EDFA compensating for the residual loss. The output SNR is fixed and set equal to 12 dB over 0.5 nm bandwidth.

Conclusions

The raise of FWM in a distributed Raman amplifier has been studied with a particular attention to the dependence of cross-talk from the pumping scheme, i.e. forward or backward pumping or a combination. Contrary to the common knowledge, the FWM cross talk has been demonstrated to be independent from the pumping scheme for non-zero-dispersion fiber (D>=2, ps/nm) and channel spacing larger or equal to 50 GHz. A hybrid system with distributed Raman amplification and concentrated EDFAs has